Performance data of the new free-piston shock tunnel at GALCIT

H. Hornung *

Graduate Aeronautical Laboratories, California Institute of Technology

Abstract

The new free-piston shock tunnel has been partially calibrated, and a range of operating conditions has been found. A large number of difficulties were encountered during the shake-down period, of which the ablation of various parts was the most severe. Solutions to these problems were found. The general principles of high-enthalpy simulation are outlined, and the parameter space covered by T5 is given. Examples of the operating data show that, with care, excellent repeatability may be obtained. The temporal uniformity of the reservoir pressure is very good, even at high enthalpy, because it is possible to operate at tailored-interface and tuned-piston conditions over the whole enthalpy range. Examples of heat transfer and Pitot-pressure measurements are also presented. The heat flux measurements were obtained on a slender pointed cone in the laminar (1 MW/m^2), and turbulent (4 MW/m^2) flow. Although the calibration of T5 is not complete, the facility has already produced important data relevant to SCRAM-jet propulsion.

1. Introduction

A free-piston shock tunnel was brought into operation at GALCIT in December 1990. The transition from the shake-down to routine operation took place in September 1991. However, further development became necessary during continued high-pressure operation because of ablation of the shock-tube wall. Facilities of this type have been in existence elsewhere for many years and a few have recently been completed. Notable examples are the tunnels known as T3 at the Australian National University, completed in 1969, T4 at the University of Queensland, completed in 1987, and HEG at the DLR in Göttingen, completed in February 1992, see Eitelberg (1992). As its name implies, T5 is in several ways a machine that has been developed from experience gained with the operation of and research in the Australian free-piston shock tunnels, all of which, starting with the very small facility T1, have served to provide scaling laws for and successive improvements in such devices, see Morrison, Stalker and Duffin (1989).

The purpose of the free-piston shock tunnel is to generate very high enthalpy flows at high density, in order to enable laboratory simulation of the chemical nonequilibrium effects encountered in the aerodynamics of transport to and from space through planetary atmospheres. The method by which the free-piston technique achieves high enthalpy at high density is to heat and compress the monatomic driver gas adiabatically with a reusable, heavy piston. The rationale leading to the technique is described by Hornung (1988).

This paper presents the features and performance data of T5 and discusses them in the light of previous results and predictions. An earlier status of T5 is presented in Hornung *et al.* (1991). Problems encountered because of extreme heat loads to the facility and their solutions are also presented.

2. Description of the facility

2.1 Dimensions, pressure levels and operation

With the constraints imposed on the design by the requirement of sufficient size and pressure for binary scaling of the important reactions, available space, safety and cost, optimization led to the following parameter values:

Maximum diaphragm burst pressure	130 MPa
Maximum secondary reservoir pressure	15 MPa
Compression tube diameter	300 mm
Compression tube length	30 m
Shock tube diameter	90 mm
Shock tube length	12 m
Piston mass	120 kg

A preliminary design to these specifications was made in December 1988.

In a typical run, the secondary air reservoir contains air at 13 MPa, the compression tube contains helium at 150 kPa, the diaphragm burst pressure is 110 MPa, and the shock tube contains 90 kPa of air. When the piston is released, it is accelerated by the compressed air to a maximum speed of about 300 m/s. The kinetic energy stored in the piston allows it to continue to move forward, thus compressing and heating the helium to around 4600 K at diaphragm rupture. The piston speed is still significant at this point, typically 150 m/s, so that the driver gas pressure is maintained approximately constant after diaphragm burst ('tuned piston' operation). With these conditions, the shock speed achieved is about 4.2 km/s, so that the specific nozzle reservoir enthalpy is about 20 MJ/kg, and the nozzle reservoir pressure is about 70 MPa.

As the piston accelerates along the compression tube, this center of mass shift is compensated by a recoil of the compression tube, shock tube and nozzle. The test section and dump tank remain stationary, and the secondary air reservoir recoils in the opposite direction under the action of the thrust of the outflowing air. To accommodate the resulting relative motions, the joints at the nozzle and at the launch manifold are fitted with sliding axial seals. The recoil speed determines the level at which the tube is stressed by a wave released by the rapid piston deceleration. This and other considerations make it desirable to reduce the recoil speed as much as possible. For this reason a substantial inertial mass (14 tons) is fixed to the

* Professor of Aeronautics and Director.
Member AIAA.

high-pressure end of the compression tube, the origin of the stress wave. The recoil distances are typically 100 mm and 150 mm for compression tube and secondary air reservoir respectively.

2.2 Instrumentation

The instrumentation available at the facility includes thermocouple type surface heat transfer sensors, piezoelectric surface pressure transducers, and Pitot pressure probes. In addition, non-intrusive visualization is routinely used in the form of differential interferometry, or schlieren photography. Instrumentation belonging to Rocketdyne division of Rockwell International Corporation and stationed at the T5 Laboratory includes high-speed video, high-speed schlieren photography (25,000 frames/s), duplicate planar laser-induced fluorescence for OH measurement, and diffuse holography.

Ancillary equipment includes a combustion-heated shock tunnel with a 1 in. diameter shock tube for synchronized hydrogen injection at speeds up to 5.5 km/s, see Bélanger and Hornung (1992), three Ludwieg tubes (property of Rocketdyne) for heated hydrogen injection at speeds up to 3 km/s, and a diaphragm indentation machine.

2.3 Data acquisition system

The modular data acquisition system consists of amplifiers, threshold detectors, digital counters (for shock speed measurement), digital delay generators (for control of test section diagnostics and hydrogen injection timing), and digitizing units. Forty A/D channels are currently available, each with a resolution of 12 bits and a maximum sampling rate of 1 MHz. The total through-put is limited to 16 MSamples/s. A typical run generates over 250 kByte of data. The system is controlled from a Sun SPARCstation computer with software facilities enabling 'quick-look' examination of the data immediately after the shot.

For image acquisition, each PLIF system is equipped with a CCD camera and accompanying software, an additional CCD camera is available for use with interferometry, and wet-film photography facilities are available.

3. Problems encountered during shake-down

The first shot of T5 was fired on December 17, 1990, and a number of difficulties were soon encountered as the operating pressure was gradually increased. The most important of these was that in the original design the secondary air reservoir was not free to recoil. The mass movement of air in the reservoir exerts a very significant thrust, however, and an extensive modification of the support system had to be designed and installed, before the pressure could be raised to design value. This work was completed in April 1991. For more detail see Brouillette (1992).

3.1 Nozzle-throat heating

The most extreme heat flux in the facility occurs at the nozzle throat. The original design used a beryllium-copper throat insert, which terminated at an area ratio of about 2. As the operating pressure of the facility was raised during shake-down, it soon became apparent that severe ablation occurred at a number of critical places. The end wall of the shock tube which was stainless steel, melted when the test gas was nitrogen and burned when the test gas was air. The liquid metal or metal oxide then flowed into the nozzle throat during the run and caused severe damage to the throat. It became clear that a different material was needed for the throat as well as for the end wall.

At first, we experimented with different materials for the throat insert. The quantity that measures the ability to withstand transient heating is the product $T_m \sqrt{\rho c k}$ (where T_m is the melting point, ρ is the density, c is the specific heat and k is the thermal conductivity of the material). Copper and molybdenum are the best materials on this scale and steel is particularly bad. Tungsten is nominally better than copper, but it burns vigorously, so much so that the diameter of the throat increases during one shot by 0.3 mm. Solid copper is too soft for the high pressures of the nozzle reservoir region. Molybdenum does a good job and is the material now in regular use. At the maximum reservoir pressure of T5, 100 MPa, the molybdenum exhibits fine hairline cracks after the second shot, which grow in width during each subsequent shot, so that the throat insert has to be replaced after 5-6 shots.

A different solution, which was found to be effective in other regions of the flow, was to electrodeposit a 0.3 mm thick layer of copper on a steel backing material. In this manner, the steel supplies the strength and the copper supplies the required thermal properties, since the penetration depth of the heat is only about 0.2 mm in the 2-3 ms of the flow duration. This method was not successful in the throat region, where the copper coating was found to melt at the point where the radius of curvature in the longitudinal plane was smallest (15mm). From this and the method of calculating throat heating rates given by Enkenhus and Maher (1963), the heat flux may be deduced to be at least 1 GW/m^2.

Downstream of the nozzle throat insert, the steel nozzle was also very severely ablated. Thus, even at area ratio larger than 3, where the temperature is already down to 0.8 times T_o, and the density to 0.2 times ρ_o, the heat flux is still well above that required to melt steel in 2 ms. A second nozzle insert was therefore made from a different material. The most successful material was found to be molybdenum, which, in that location does not crack, even at the highest operating pressure. It does not require replacement.

3.2 Ablation in other regions

The melting and burning of the shock tube end and side walls in the nozzle reservoir region could be prevented by using copper-coated inserts up to a distance of 8 shock tube diameters upstream from the end wall. The shock tube wall inserts required the last shock tube segment to be removed and taken to a machine shop since it had to be bored out. The insert is made of stainless steel with a 0.3 mm thick copper coating on the inside and a steel wall thickness of 10 mm. The end wall surrounding the throat insert is also made in this way. All the inserts have to be able to seal vacuum and high pressure, of course, so that a total of 6 additional 'o'-ring seals were required.

At this time, there remains one place where ablation is still occurring. This is just downstream of the diaphragm, where the shock tube diameter decreases in a step in order to prevent the diaphragm petals from being picked up and bent back by the reflected shock. The step presents a steel obstruction to the flow, at which significant ablation takes place. This will be replaced by a copper step in the near future, and it is expected that this will solve the problem.

3.3 Piston seals

The rear piston seal is made of nylatron. The sealing action relies on the air pressure behind the piston to deflect a thin skirt of nylatron against the inner surface of the compression tube. It turned out that this seal exhibited excessive wear at high pressure conditions, and had to be redesigned to have a somewhat stiffer flexible element, see Brouillette (1992) for more detail.

A more severe problem was encountered with the front seal on the piston. This employs a chevron ring principle, the original design being shown in Fig. 1. The aluminum-bronze ring has 4 small holes that communicate the high-pressure helium to a small cavity between itself and the nylatron chevron sealing ring. The idea is that the pressurization of the chevron ring from the inside will push it against the compression tube wall, thus sealing against the helium. Unfortunately, the cavity will then leak to the space between the piston body and the tube wall, with the consequence that the heat transfer (in the presence of fast flow) becomes excessive, and the aluminum-bronze ring melts near the 4 holes. A second problem that occurred during the off-design conditions that were being run during shake-down, was that the aluminum-bronze ring could fail, either by twisting off in a forward direction, or by shearing off the aluminum threads of the piston.

Modifications were made to the design in a number of steps, that led to the design shown in Fig. 2. The aluminum spacer ring was replaced by a thicker steel ring and the aluminum-bronze ring was extended to the back to be constrained by the new steel ring in order to prevent it from lifting off the thread, thus preventing it from twisting off. A piece of the piston was removed and replaced by a hardened steel piece screwed onto the piston, such that the aluminum-bronze ring would fail in thread shear first. These two modifications were successful in preventing failure of the ring. The seal was redesigned by adding the two 'o'-rings shown in Fig. 2, which now prevent any leakage out of the cavity and completely remove the problem. The seal now works very well, no blow-by or melting has been occurring with it at all.

3.4 Transducer amplifiers

One of the features of modern electronic miniaturization was that the impedance converters of piezoelectric pressure transducers could be made so small, that they could be housed in the body of the transducer. This has the disadvantage in the environment of T5, that the circuit is subjected to higher acceleration than it can survive re-

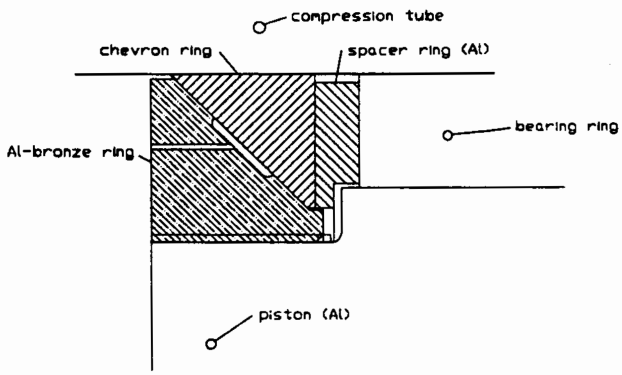

Fig. 1 Original design of front piston seal

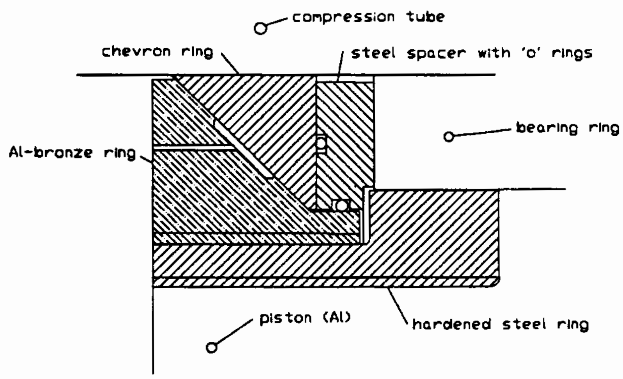

Fig. 2 Modified design of front piston seal

peatedly. It was necessary to revert to the earlier designs, where the impedance converters were placed in the cable a short distance from the transducer, so that they could be isolated from the acceleration.

4. Performance

4.1 High-enthalpy flow simulation

At high enthalpy, the Mach number, which measures the square root of the ratio of the ordered kinetic energy of the flow to the thermal energy of the gas, is not so important as the ratio of the ordered kinetic energy measured in terms of the specific dissociation energy of the gas. There are usually several such characteristic chemical energies. The characteristic specific energies relevant for air are

$$\begin{aligned} D_{N_2} &= 33.6\,\mathrm{MJ/kg} & E_{vN_2} &= 0.992\,\mathrm{MJ/kg} \\ D_{O_2} &= 15.5\,\mathrm{MJ/kg} & E_{vO_2} &= 0.579\,\mathrm{MJ/kg} \\ D_{NO} &= 20.9\,\mathrm{MJ/kg} & E_{vNO} &= 0.751\,\mathrm{MJ/kg}\ . \end{aligned}$$

where the D's and E_v's are specific energies of dissociation and of vibration respectively. It is therefore not possible to simulate the numerous idiosyncrasies of a particular gas by using another gas. Thus, the specific chemical energies have definite known values, and the duplication of the ratios of the ordered kinetic energy to them in a simulation implies that the actual flow speed has to be duplicated.

It follows that the reservoir enthalpy h_0 of the flow, which is approximately equal to $V^2/2$, where V is the flow speed, has to have the same value as in flight. If the flow is accelerated from rest, as in T5, the reservoir enthalpy corresponding to, say, a flow speed of 6 km/s is 18 MJ/kg, which, at a reservoir pressure of 100 MPa, implies a temperature of nearly 9000 K in air.

The high pressure is necessary to ensure that the chemical reaction rates occur at the right rate for correct simulation of nonequilibrium effects. Smaller scale requires faster reaction for correct simulation. If the temperatures are right (as is ensured by correct flow speed) the reaction rates depend mainly on the density. Rates for binary reactions, like dissociation, are linear in density, those for three-body reactions like recombination are quadratic in density. Thus, all reactions can never be simulated correctly except at full scale. In many cases, three-body reactions are not important and where they are, component testing or extrapolation is necessary.

Two difficulties arise in simulation of high enthalpy flows in reflected shock tunnels: The nozzle expansion is not able to fully recombine the gas to the undissociated condition of free flight, and the Mach number of the flow is lower than that of free flight (free stream temperature too high) unless the nozzle area ratio is extremely high. The latter is precluded by the need for sufficiently high density, unless the pressure is increased enormously. This in turn introduces even more severe heating problems than were encountered in T5. (A facility in which the reservoir pressure will be an order of magnitude higher than in T5 is under construction at AEDC, see Maus *et al.*, 1992).

Thus the parameters of interest in the assessment of a facility's ability to simulate high enthalpy flows are the ranges of flow speed, density and size, as well as the free stream composition, Mach number and test time. Much is often made of the last of these, and the question of whether it is sufficiently long. Experience with T5 has clearly demonstrated that under no circumstances should the test time be increased, if the facility is not to be destroyed by ablation. Also, that the steadiness of the flow over typically 2 ms has been demonstrated by schlieren movies to be very good (Experiments by Rocketdyne in T5).

4.2 Parameter space of T5 performance

In the characterization of a facility's performance, it is essential that parameter values are quoted in context. For example, it is not sufficient to say that the specific enthalpy ranges up to 20 MJ/kg, unless the values of the density and Mach number are also quoted. Thus, while arc-heated tunnels can produce this specific enthalpy, the density is so low that no significant recombination occurs in the nozzle flow, and the reaction rates behind a normal shock are far too slow. In the case of shock tunnels which use steady heating of the driver gas so that the the driver temperature is limited to 750 K, high specific enthalpy can only be achieved at low density. Consequently, the reaction rates are again too slow. For comparison, the free-piston shock tunnel typically operates at driver gas temperatures of 4500 K. It is also necessary to relate the size, Mach number and free-stream composition to these parameters.

4.2.1 Binary scaling, enthalpy, free-stream freezing

Following the arguments in the previous section, the best way to display the performance of a high-enthalpy facility is in a plot of the product of density ρ and nozzle exit diameter d against the square root of specific reservoir enthalpy. For a given gas, the density-length product characterizes the binary reaction rates, and $\sqrt{(2h_0)}$ characterizes the equilibrium behavior. Such a representation is given for T5 in Fig. 3. On the abscissa of Fig. 3, three arrows mark values of some of the specific dissociation and vibration energies of air components. The top straight line defines the upper boundary of the range of conditions achievable by T5 with a reservoir pressure of 100 MPa and with a 32 mm diameter throat, at an area ratio of 100. The lower straight lines represent the upper limits for the same throat diameter but larger exit diameters, and correspondingly longer nozzles. Such larger nozzles do not at present exist.

To compare with these performance limits, the figure also shows the trajectories of the National Aerospace Plane on ascent and reentry. For this comparison, it was assumed that the span of a model would be equal to half the exit diameter of the nozzle. Fig. 3 also shows the values of the atomic oxygen concentration as a mass-percentage at different points of the present nozzle flow in air. The atomic nitrogen concentration is negligible at specific enthalpies below 25 MJ/kg, or at equivalent speed below 7 km/s. The larger nozzles indicated in Fig. 3 would require some hardware modifications, but otherwise present no new problems. At any condition on or below the straight line, it is possible to operate T5 with tailored interface conditions. This is achieved at the lower enthalpies by mixing various amounts of argon with the helium driver gas. In this way the speed of sound of the driver gas can be changed over a much wider range than is easily achievable by changing the compression ratio of the piston compression. Very low densities can only be achieved by reducing the throat

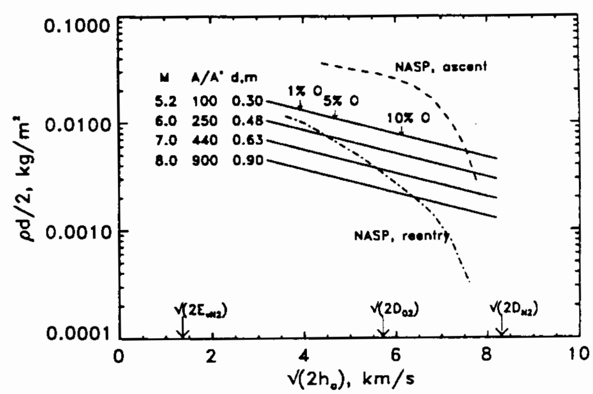

Fig. 3 T5 performance limits in relation to NASP trajectories and air properties for the existing (M=5.2) nozzle and possible other nozzles at nominal Mach numbers as indicated. The free-stream atomic oxygen concentration is shown as a mass percentage.

diameter, which involves operating the present nozzle off design.

The upper straight line of Fig. 3 is based on experimental results such as measurements of shock speed, reservoir pressure, Pitot pressure, heat flux, and flow visualization.

No measurements of gas composition have been made so far. The gas composition quoted in the form of atomic oxygen concentration is based on nonequilibrium axisymmetric nozzle-flow computations using the SURF code (see Rein, 1990, 1991, 1992). However, computations show that the sensitivity of the exit composition to the reaction rates is small compared with the uncertainties in the rates, so that these concentrations can be regarded with some confidence. Previous experience with mass-spectrometric measurements by Crane and Stalker(1977) support this view. The Pitot pressure measurements indicate that the nozzle-wall boundary layer has a very small displacement thickness in the Mach 5.2 nozzle. The other straight lines in Fig. 3 are based on approximate extrapolation and numerical computation with SURF.

The low Mach number nozzle is particularly useful for SCRAM-jet combustor testing, because the inlet conditions for these can be duplicated almost exactly for the NASP ascent. This is the reason for the extended tests that have been performed in T5 by Rocketdyne, see Davis *et al.* (1992), also Waitz *et al.* (1992). In these experiments, the steadiness of the flow was demonstrated by time-resolved (movie) schlieren photography, and successful PLIF measurements of OH concentration were obtained with synchronized hydrogen injection.

4.2.2 Test time

An important parameter of shock tunnel operation is the test time before driver-gas contamination. So far, only an indirect method has been used to measure this time. It employs the phenomenon of shock detachment from a wedge. The detachment angle for the exit conditions with dissociating nitrogen is approximately 46 deg., and with monatomic gas is approximately 36 deg. Thus, if a 45 deg. half-angle symmetrical wedge is placed in the flow, the shock will be attached while the flow consists of test gas, and will detach, when the monatomic driver gas arrives. This technique will, of course, not detect very low concentrations of driver gas, but is a useful indicator of the approximate arrival time of driver gas. In order to make it a little more sensitive, the quantity s, see Fig. 4, was measured as a function of time. For approximately 3 ms, s remains fairly constant indicating no contamination and rises in an erratic fashion thereafter, until, at 4-5 ms, the flow breaks down completely. The model for this flow was just a piece of angle iron, rigged up quickly at a time when a few runs became available to do this test. Clearly, more sophisticated contamination measurements are still needed.

Fig. 5 shows a diagram giving the test time as a function of reservoir enthalpy, as predicted after the preliminary design was completed in December 1988. The limit to the test time is the arrival of the driver gas. The limited amount of data available so far indicates that the curve in Fig. 5 gives a very conservative estimate. The constancy of the reservoir pressure in T5 is very good during this period, because it is being operated at tuned piston and tailored-interface conditions. At the maximum pressure of 130 MPa (diaphragm burst), the piston is not heavy enough to give optimum constant-pressure duration. A heavier piston has been designed and is awaiting funding. This will also enable more satisfactory lower compression ratio operation.

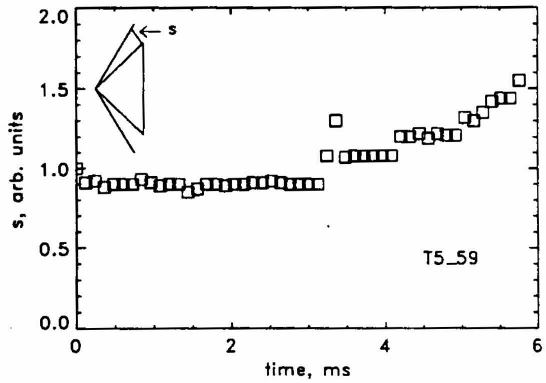

Fig. 4 The shock on a 90 deg. wedge as an indicator of contamination onset. The distance s increases significantly as the monatomic driver gas arrives. These measurements were made with a high-speed schlieren system by Rocketdyne, see Davis *et al.* (1992).

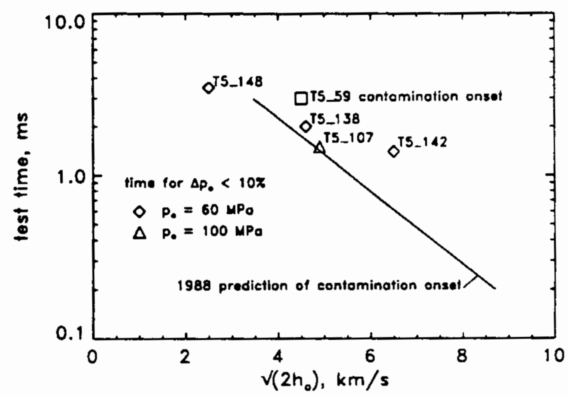

Fig. 5 Measured quantities relating to the available test time, compared with predicted contamination onset. This prediction appears to be conservative.

4.3 Examples of T5 operating conditions

In order to illustrate the quality of the T5 operating conditions, a few representative data are collected in this section. One of the important qualities of such a facility is the repeatability of the shock speed. The shock speed, V_s, depends on the thermodynamic state of the three gases before the shot and the diaphragm burst pressure. The temperature and pressure of the air driving the piston, the driver gas, and the test gas, the driver-gas mixture ratio, and the diaphragm burst pressure make 8 variables, each of which is only repeatable within an experimental error. To illustrate how well V_s can be repeated, the table shows the results of 5 successive shots with nominally equal conditions. As may be seen, the variation of V_s is less than 1%. It needs to be pointed out that V_s varies by a larger amount than this over the length of the shock tube in one shot, as a result of the attenuation caused by the turbulent boundary layer on the shock tube wall. The values given in Table 1 are measured at the second-last shock-timing interval.

It should also be pointed out here that the free-piston driver is significantly different from the usual long driver without area change, as on a conventional shock tube. The proximity of the piston to the diaphragm station and its speed mismatch and acceleration cause weak waves to follow the shock and to modify its strength. It is therefore very important to operate with tuned-piston conditions, as has been shown by the method-of-characteristics computations of Hornung and Bélanger, 1990.

The good repeatability of the diaphragm burst pressure, on which the repeatability of V_s also depends, is achieved by using the diaphragm indenting machine for preparing the diaphragms. This also produces diaphragms much more cheaply than other methods. It is based on a configuration suggested to the author by Lucien Dumitrescu in 1991 and is described in detail by Cummings (1992). By weighing the diaphragm before and after the shot, the material loss was determined to be about 100 mg.

shot no.	V_s, km/s	p_0, MPa
140	4.76	57
141	4.72	55
142	4.76	58
143	4.74	60
144	4.78	60

The second quantity that needs to be accurately known and repeatable is the nozzle reservoir pressure. To illustrate the character of the reservoir pressure trace, Fig. 6 shows a number of such traces for the corresponding shots of the table. As may be seen, at this enthalpy and pressure, the reservoir pressure p_0 is virtually constant over a period of about 2 ms. These shots are very close to the tailored-interface condition, as may be seen from the traces. The value of p_0 is also given in the table. As may be seen, the repeatability of p_0 is within $\pm 4\%$. Very careful setting up is required to obtain these accuracies. V_s and p_0 are the two quantities that determine the equilibrium reservoir state of the test gas.

In order to illustrate how tailored-interface operation is possible at different enthalpies, Fig. 7 shows two p_0 traces at different values of h_0. The free-piston machine permits tailoring over the full range of h_0 as well as over the full range of p_0. The latter in the case of T5, is from 20 to 100 MPa. The lower limit is again related to the piston mass. With a lighter piston, p_0 could be further reduced.

The Pitot pressure survey that has been made in T5 suffered from the fact that the Kulite gauges that were used for this purpose did not survive the thermal and shock load at the maximum-pressure conditions at which they were taken. The limited data available are shown in a plot of Pitot pressure against radius in Fig. 8. Also shown is the numerically computed value of the radial distribution. These results were taken only at one axial position, and at a time when the nozzle ablation problem was most severe. They clearly need to be repeated much more thoroughly and with better instrumentation. Nevertheless, the values lie in the range where the SURF code predicts them for the corresponding range of p_0 variation. A new set of probes for the Pitot rake, using piezoelectric pressure sensors, is presently being designed.

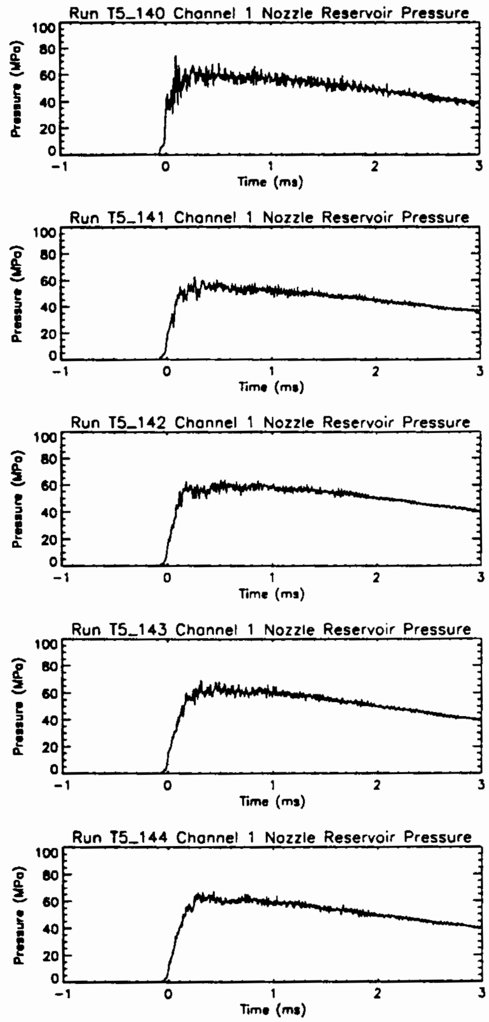

Fig. 6 Nozzle reservoir pressure traces of 5 consecutive shots with nominally the same conditions, $h_0 = 22\,\mathrm{MJ/kg}$.

A large number of heat transfer measurements was made in the test series of Rocketdyne. These used thermocouple sensors which were found to withstand the conditions in T5 without problems. A project now under way studies the transitional boundary layer on a slender cone. It was originally planned to use home-made thin-film heat flux gauges, but these were obliterated by the flow in very few runs. We therefore also switched to the thermocouple sensors.

A couple of examples of such measurements, one in the laminar, and one in the turbulent part of the boundary layer on a 5 deg. half-angle cone, are shown in Fig. 9. These were taken at a specific reservoir enthalpy of $h_0 = 12\,\mathrm{MJ/kg}$. The raw-data surface temperature trace is deconvolved to generate the integrated heat flow per unit area, which is then differentiated to give the heat flux. No smoothing is applied in this process. The differentiation of experimental data makes the traces very noisy, but the quality of these may be regarded as very good in the context of high-enthalpy shock tunnel measurements. Great care was necessary to shield from the electrical noise generated by the hot flow.

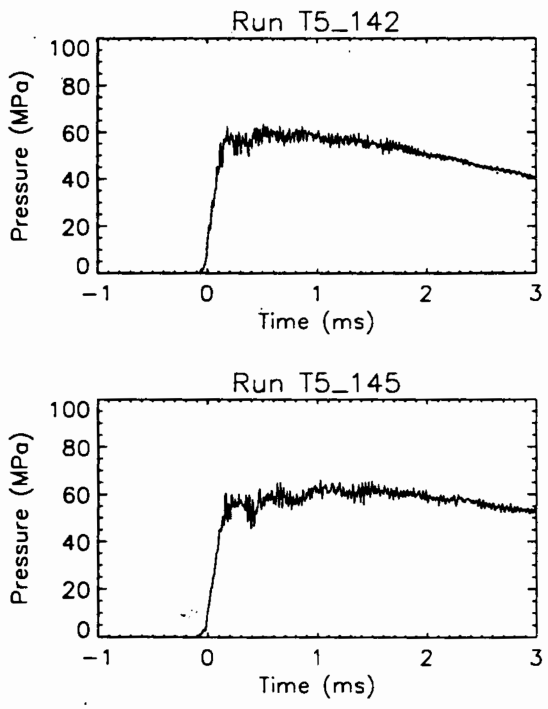

Fig. 7 Nozzle reservoir pressure traces of shots 142, and 145 at 22 and 11 MJ/kg, respectively.

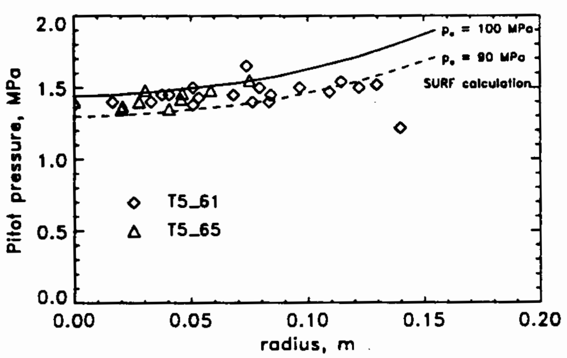

Fig. 8 Radial distribution of measured Pitot pressure 126 mm downstream of the exit plane of the nozzle. h_0 = 12 MJ/kg, p_0 between 90 and 100 MPa. The lines show results of inviscid, axisymmetric, nonequilibrium computations using SURF. The outermost point lies in the expansion fan originating at the nozzle edge.

Note that the heat flux, even on a slender cone, reaches more than 4 MW/m^2 just after transition, which is more than 4 times the value in the laminar boundary layer just before. It is also important to note that the mean value within the higher frequency noise is approximately constant for 2 ms. For more detail, including visualization of transitional flow and transition Reynolds numbers, see Germain and Hornung (1992).

5. Conclusions

The performance and shake-down history of the free-piston shock tunnel T5 is presented in some detail. The parameter range achievable, the limitations, and some results are given.

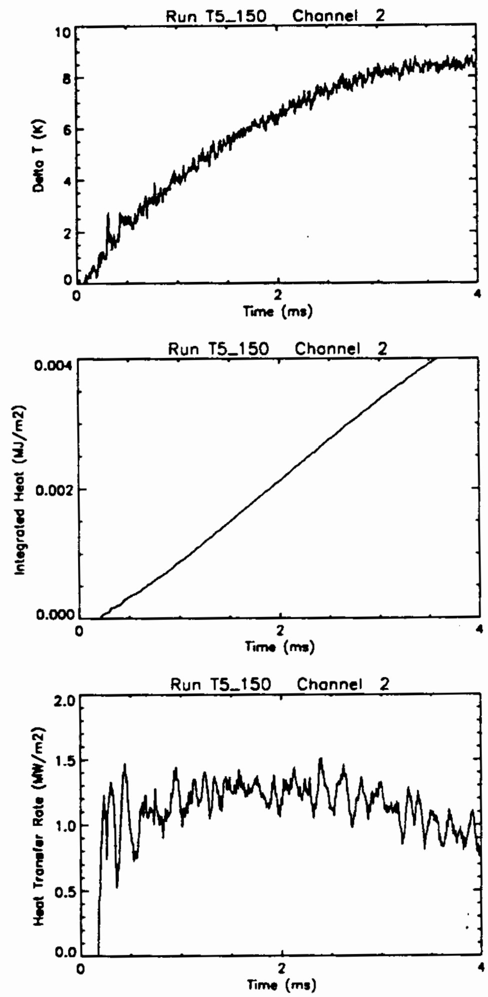

Fig. 9 Heat transfer measurement on a 5 deg. half-angle cone, laminar boundary layer, h_0 = 12 MJ/kg; upper trace: surface temperature, middle trace: heat flow per unit area, lower trace: heat flow rate per unit area.

T5 has so far been used mainly for a dedicated combustor experiment by Rocketdyne, which is not reported on here. Our own research results are therefore limited at this stage. However, the performance data so far show that the conditions achieved in the facility are as had been predicted or better, and the quality of the flow is very good. To some degree this is because the flexibility of the free-piston machine, which allows it to be operated at tailored-interface condition over the full specific reservoir enthalpy and reservoir pressure ranges, is fully exploited. T5 is also being operated at tuned-piston conditions, which gives longer constant pressure duration. Test flow calibration results also show better performance than predicted. More extensive test flow calibration is still needed.

T5 has been demonstrated to fill an important gap in the range of ground testing facilities. With further enhancement of the instrumentation and further trimming of the operation, the value of this national resource will be further increased.

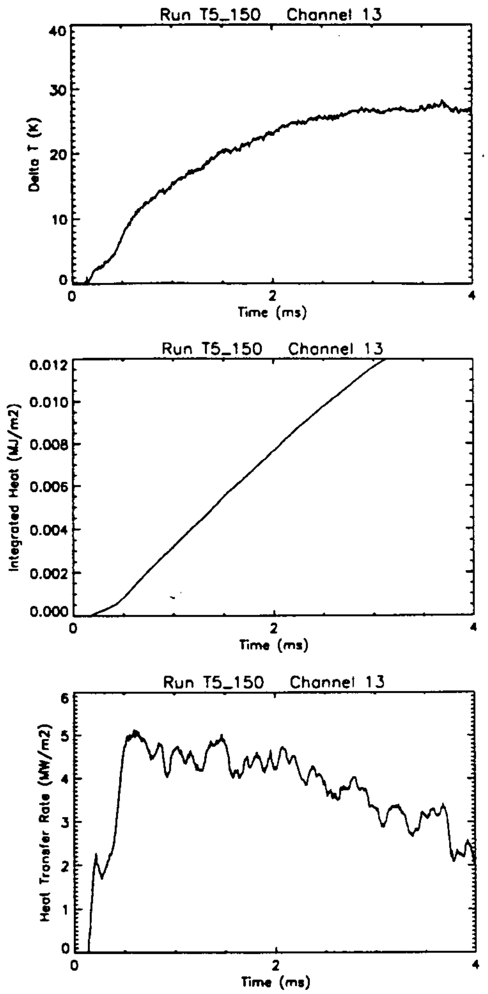

Fig. 10 Heat transfer measurement on a 5 deg. half-angle cone, turbulent boundary layer, in the same flow as that of Fig. 9, but further downstream.

6. Acknowledgments

This work was supported by ONR Grant N00014-90-J-1305, and NASA Grant NAG-1-1209.

We would also like to thank Rocketdyne Division of Rockwell International Corporation for manpower support, particularly by Darlene Gieseking, and for use of their high speed schlieren system as well as the thermocouple sensors.

T5 is a team effort: Jacques Bélanger, Martin Brouillette, Eric Cummings, Patrick Germain, Hans Hornung, Simon Sanderson, Brad Sturtevant, Bahram Valiferdowsi, and Chih Yung Wen.

7. References

Bélanger, J. and Hornung, H. 1992 "A combustion driven shock tunnel to complement the free piston shock tunnel T5 at GALCIT", AIAA 92-3968, Nashville.

Brouillette, M. 1992 "Design modifications to T5 and their implementation", GALCIT Report FM 92-3.

Crane, K. C. A. and Stalker, R. J. 1977 "Mass-spectrometric analysis of hypersonic flows," *Journal of Physics D: Applied Physics*, **10**, 679-695.

Cummings, E. 1992 GALCIT report, in preparation.

Davis, J.A., Hornung, H., Campbell, R. L. and Medley, J. A. 1992 "Performance of the T5 free-piston shock tunnel at Caltech", NASP Mid-term Technology Review, Monterey, CA.

Eitelberg, G. 1992 "The high-enthalpy shock tunnel in Göttingen", AIAA 92-394 2, Nashville.

Enkenhus, K. R. and Maher, E. F. 1963 "The aerodynamic design of axisymmetric nozzles for high-temperature air", Naval Ordnance Laboratory, White Oak, MD, NAVWEPS Report 7395.

Germain, P. and Hornung, H. 1993 In preparation.

Hornung, H. 1988 "28th Lanchester memorial lecture - Experimental real-gas hypersonics", *Aeron. J.*, Dec. 1988, p.379, see also *Z. Flugwiss. Weltraumf.* **12**, p. 293.

Hornung, H. and Bélanger, J. 1990 "Role and techniques of ground testing for simulation of flows up to orbital speeds", AIAA 16th Ground Testing Conf. Seattle, AIAA 90-1377.

Hornung, H., Sturtevant, B., Bélanger, J., Sanderson, S., Brouillette, M. and Jenkins, M. 1991 "Performance data of the new free-piston shock tunnel T5 at GALCIT", *Proc. 18th Int. Symp. on Shock Waves*, Sendai, Japan.

Maus, J. R., Laster, M. and Hornung, H. 1992 "The G-Range impulse facility - a high performance free piston shock tunnel", AIAA 92-3946, Nashville.

Morrison, W. R. B., Stalker, R. J. and Duffin, J. 1989 "New generation of free piston shock tunnels", *Proc. 17th ISSWST*, Bethlehem, PA. p. 582.

Rein, Martin 1989 "SURF: A program for calculating inviscid supersonic reacting flows in nozzles", GALCIT Report FM 89-1.

Rein, Martin 1991 "Partial chemical equilibrium: Theory and implementation in the program SURF", GALCIT Report FM 91-1.

Rein, Martin 1992 "The partial equilibrium approximation in reacting flows", *Phys. Fluids A*, 4, 873-887.

Waitz, Ian *et al.*1992 In preparation.